Microwave measurement of electrical fields in different media – principles, methods and instrumentation

Plamen I. Dankov

Sofia University "St. Kliment Ohridski", Faculty of Physics, James Bourchier blvd., Sofia 1164, Bulgaria

E-mail: dankov@phys.uni-sofia.bg

Abstract. This paper, presented in the frame of 4th Int. Workshop and Summer School on Plasma Physics (IWSSPP'2010, Kiten, Bulgaria), is a brief review of the principles, methods and instrumentation of the microwave measurements of electrical fields in different media. The main part of the paper is connected with the description of the basic features of many field sensors and antennas – narrow-, broadband and ultra-wide band, miniaturized, reconfigurable and active sensors, etc. The main features and applicability of these sensors for determination of electric fields in different media is discussed. The last part of the paper presents the basic principles for utilization of electromagnetic 3-D simulators for E-field measurement purposes. Two illustrative examples have been given – the determination of the dielectric anisotropy of multi-layer materials and discussion of the selectivity of hairpin-probe for determination of the electron density in dense gaseous plasmas.

1. Introduction

The determination of the high-frequency electrical (E) fields is not a primary type of measurement in the microwave range like the measurements of power, frequency, spectrum, device's S-parameters and noise. In fact, the local E-field magnitude around a given radiator or in a given electro-magnetic (EM) media could be determined by the same equipment for measurements of power, spectrum and S-parameters – power meters, spectrum analyzers and network analyzers. A necessity to obtain an actual information about the E-field intensity, orientation and distribution appears for three basic groups of measurement: 1) EMC/EMI measurements (electromagnetic compatibility/interference); 2) antenna measurements (mainly for communication purposes) and 3) characterization of different materials and media (crystals, reinforced substrates, liquids, powders, absorbers, thin films, biological tissues, gaseous plasmas, etc) and imaging. The EMC/EMI measurements will not be considered here; they are very important in the communications and for determination of the safety standard for non-ionisating radiation [1]. We will focus our discussions here on the main principles, methods and instrumentation of the E-field measurements; the variety of E-field sensors and their implementation and finally, on the utilization of the modern EM 3-D simulators as an assistant tool for measurement purposes.

2. Electrical-field measurements' principles and instrumentation

2.1 Measurement principles

Let us start with the discussion of figure 1, where the conditional scheme of the E-field measurements is presented. The unknown signal falls over a sensor or an antenna and the equivalent response after a conversion (into dc, RF or IR power; or directly) is received and the detected signal is displayed. This
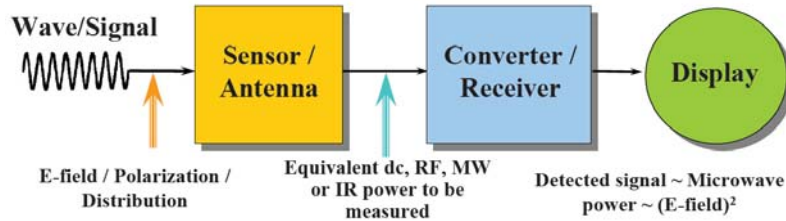
Figure 1. Conditional block scheme for measurement of high-frequency electric fields.

displayed response is usually proportional to the microwave power (or E-field square). The basic power sensors are the well-known termistors, thermocouples and diode detectors [2]. In the next section we will focus our attention to the description of variety of E-field probes and antennas as an effective receiving equipment for determination of the local E field and imaging.

There exist three basic methods for receiving of the unknown signal – see figure 2. The simplest way is the power detection. The detector converts the radio-frequency (RF) power into an equivalent dc or low-frequency (1-100 kHz) current/voltage. The sensitivity is not high – the minimal detecting power is ~ 10^{-7} mW (or –70 dBm) and the dynamic range between the maximal and minimal receiving power is typically 30-40 dB up to 70 dB. More effective is the down-conversion (or mixing), where the unknown signal is mixed with a controlled signal by a local oscillator (LO) and the response is measured at the intermediate frequency (IF) – typically several hundred MHz. The response could be digitalized by analog-to-digital converter (ADC) and then treated by a digital signal processing (DSP). The main benefit of the mixing is that the IF frequency falls into the frequency range, where the noise components is formed mainly by the thermal noise and the low-frequency $1/f$-noise does not appear. Thus, the sensitivity increases – the minimal detecting power is now ~10^{-12} mW (or –120 dBm) and the dynamic range increases up to 100-110 dB. The biggest sensitivity and dynamic range (~140 dB) can be achieved by the sampler – here the LO is a frequency synthesizer, which produces a fixed array ("comb") of LO-frequencies with high enough levels, stable amplitudes and frequencies.
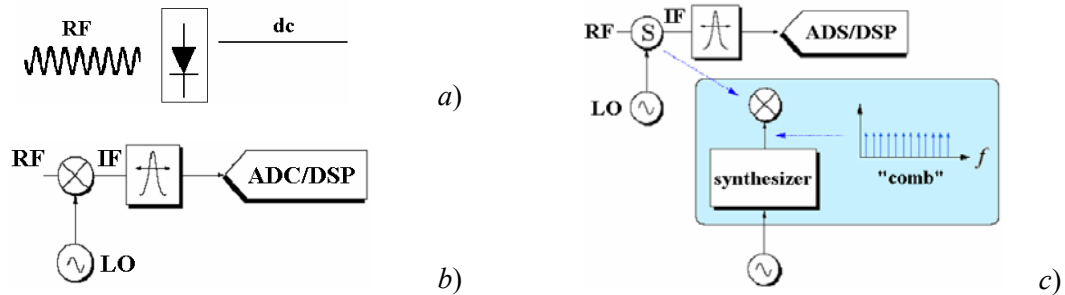

Figure 2. Three basic methods for receiving the signals: *a*) by a detector; *b*) by a mixer; *c*) by a sampler.

2.2 Main measurement schemes

Figure 3 illustrates three basic schemes for determination of the E fields. When the media under test (MUT) produces own RF fields, the simplest scheme consists of a receiving antenna (probe) A_R and a spectrum analyser SA (preferable highest sensitivity tool) or wattmeter W (cheaper tool with lower sensitivity). This scheme is applicably also for "near-field" scanning/imaging. If the MUT is passive, it could be illuminated by a known RF signal (A_T) and the response signal (A_R, A_T) (transmitted and/or reflected) will be a measure of the MUT dielectric properties. This case, known as a "free-space" method, is applicable using network analyzer NA [3]. The most sensitive way to determine the dielectric properties is the resonance method – now the MUT is a resonator itself (or its filling) and the field response is a good measure of the material properties of this media using NA. Figure 4 illustrates the combination of the necessary equipment (W, SA and NA) – the "dream" of each RF engineer.

Finally, let us discuss the measurement strategy. It is important to note, that the power-flux density $\bar{S}$ is the basic "measurable" parameter in the microwave range. If $\bar{S}$ is known (measured), the necessary
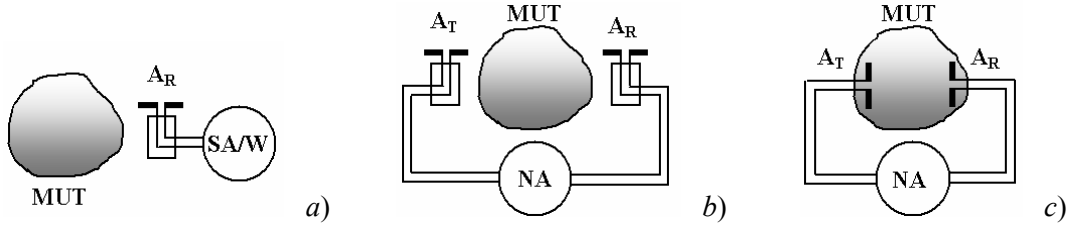
Figure 3. Three basic measurement schemes for determination of the E fields in a media under test (MUT) ($A_{T,R}$ – transmit/receive antennas): *a*) characterization of the own transmitted fields in MUT by SA (spectrum analyser) or W (wattmeter). This application is very suitable also for "near-field" scanners; *b*) illumination of MUT and measurement of the field response by NA (network analyser) – "free-space" method; *c*) MUT as a resonator – characterization of its dielectric properties of MUT

Figure 4. Basic measurement equipment: *a*) wattmeter W; *b*) spectrum analyser SA; *c*) network analyser NA

averaged fields $\overline{E}$ and $\overline{H}$ can be easy expressed through $\overline{S}$ for plane waves using the expressions (1, 2) (see figure 5*a*). A direct measurement of the E field is also possible, when the antenna factor *AF* of the measurement antenna is known – see figure 5*b*. The antenna factor is the ratio of incident local E-field intensity E_{local} (upon the antenna) to the measured voltage V_{meas} that is produced at the antenna terminal – a 50-ohms load. If the test antenna is reference, the frequency-dependent parameter *AF* is usually given by the manufacturer; if not, the *AF* can be derived from the antenna gain *g* using the expression (4). The unknown antenna gain *g* can be easy obtained by the known two-antenna method – see figure 5*c*. Two equal antennas – receiving and transmitting, are placed at a distance *d*, which is greater than the so-called "far-field-zone" radius R_{ffz} of the antenna – equation (6). If the both antennas

$$\overline{S} = 0.5\,\text{Re}(\mathbf{n}.\vec{\mathbf{S}}) = 0.5\,\text{Re}(E_p \times H_p^*)_z = \text{Re}(\overline{E}_{rms} \times \overline{H}_{rms}^*)_z \quad (1)$$

$$\overline{E} = 19\sqrt{\overline{S}}, \text{V/m}; \quad \overline{H} = 4.8 \times 10^4 \sqrt{\overline{S}}, \text{A/m}; \quad \overline{S}, \text{W/m}^2; \quad (2)$$

$$E_{local}, \text{V/m} = AF, 1/\text{m} \times V_{meas}, \text{V} \quad (3)$$

$$AF(f), 1/\text{m} = 9.73/(\sqrt{g}\,\lambda_0, \text{m}) \quad (4)$$

$$g - \text{antena gain as a ratio}$$

$$P_R = P_T g_T g_R (\lambda_0/4\pi d)^2 \quad (5)$$
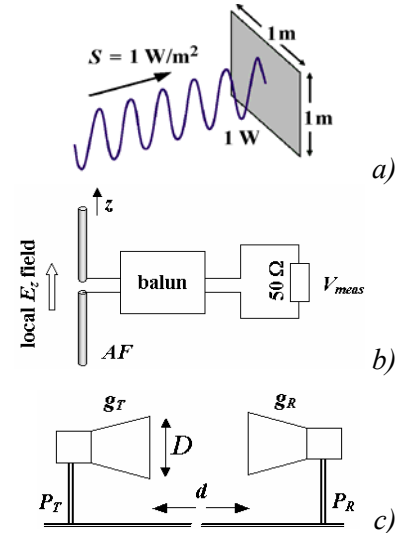
$$d > R_{ffz} = 2D^2/\lambda_0 \quad (6)$$

Figure 5. Basic relations between the average power-flux density $\overline{S}$, average E-field intensity $\overline{E}$ and average magnetic (H-) field intensity $\overline{H}$. Denotations: E_p, H_p – peak-amplitude fields, E_{rms}, H_{rms} – "root-mean-square" fields, known also as average or effective ("measurable") fields; E_{local} – local E field; *AF* – antenna factor; g – antenna gain; $P_{T,R}$ – transmitted/received power; λ_0 – wavelength; *d* – distance between the antennas; R_{ffz} – antenna far-field zone radius; *D* – antenna diameter/dipole length

are equal, their common gain $g = g_T = g_R$ can be calculated using the equation (5), if the transmitted P_T and received power P_R have been measured. Thus, the presented equations (1-6) can help practically in each situation for E-field measurement.

3. Field sensors
In this section we discuss the variety of field sensors, probes and antennas for receiving of the signal. The discussion includes mainly the problems how to do sensors broadband, miniaturised and tuneable. This is not a full description – only the well-known and some modern solutions have been given.

3.1. Simple dipoles, monopoles and apertures
The simplest way to "see" the local E field in a given place is the wire probe. Figure 6 *a*, *b* illustrates the most spread field sensors [4, 5] – dipoles and monopoles from electric (open wires) and magnetic (loops) types. The length of the dipoles is usually chosen $\sim\lambda_0/2$, while the length of the monopole is $\sim\lambda_0/4$, but this is not a rigorous rule (the monopole is half of dipole placed on top of a ground plane). Contrariwise, if the length of the used probe is $D \langle\langle \lambda_0/2$, this is a typical local sensor for detecting the field, nevertheless its small sensitivity. The strongest signal in the feed lines appears, if the E-probe is parallel to the E field direction, or if the H-probe loop plane is perpendicular to the H field. A popular example is illustrated in figure 7 for excitation of the TE_{011} mode in the dielectric resonator – two positions of the E- and H-probes are given, for which this mode could be (or could not be) excited.

If the length of the dipole wires is $\lambda_0/2$, the probe becomes resonance (see figure 8) and the current response in the centre increases. The gain of similar probe is ~1.64; for example, using expression (4) for resonance dipole at 2.45 GHz the antenna factor AF is 62.06 1/m or 35.85 dB/m. Increasing the dipole length, the distribution of the induced current changes and the concept of the radiation pattern should be introduced (Figure 9a). The definition of the radiation pattern is the normalized E-field distribution $F(\varphi,\theta) = E(\varphi,\theta)/E_{max}$ according to the azimuthal and elevation angles to the maximal field.
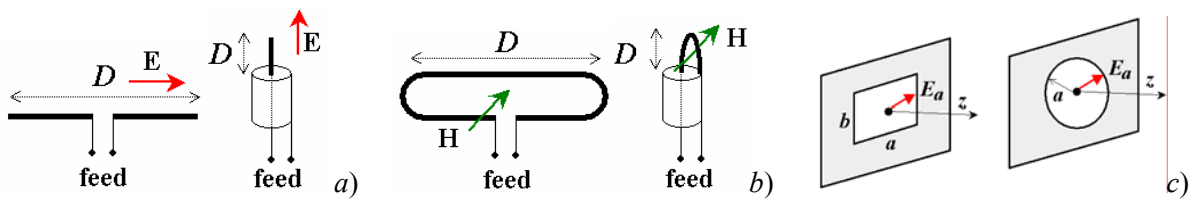

Figure 6. Simples field sensors: *a, b*) E- and H-field dipole and monopole; *c*) Huygens' apertures ($a.b \langle\langle \lambda_0^2$)
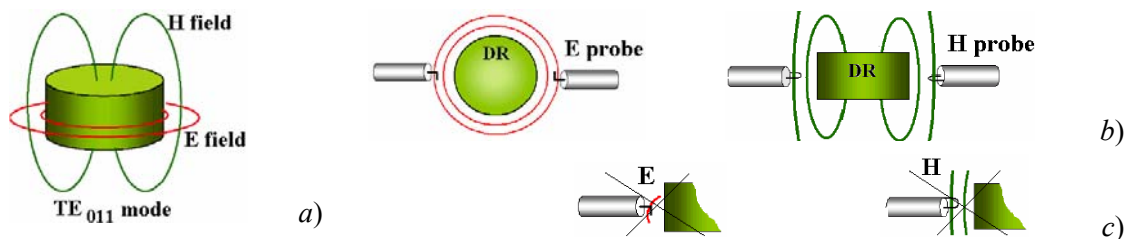

Figure 7. Example for excitation of the TE_{011} mode of the dielectric resonator DR by local E- or H-type probes: *a*) mode fields, *b*) the TE_{011} mode is excited; *c*) the TE_{011} mode is not excited.
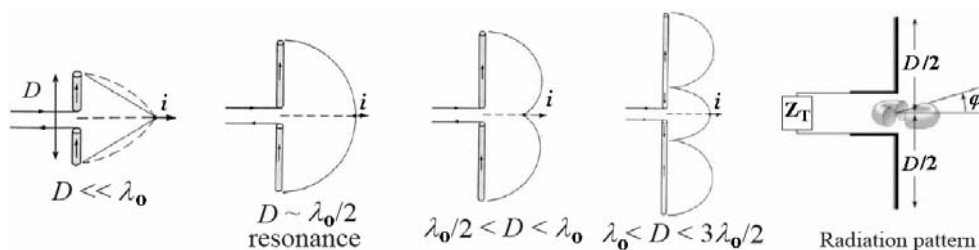

Figure 8. E-field dipole with increasing length and introduction of the concept for the radiation pattern [4]
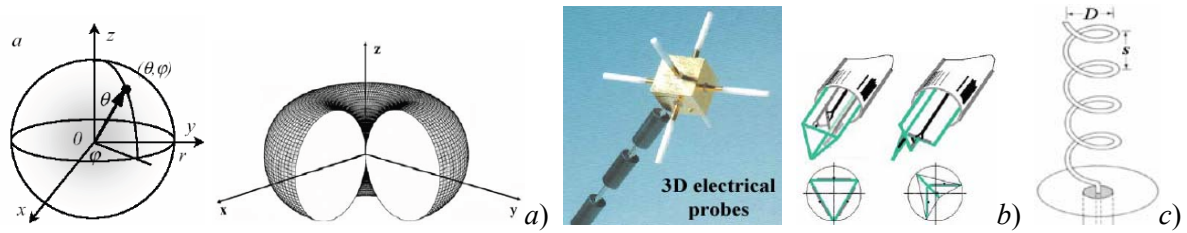
Figure 9. *a*) Azimuthal φ and elevation θ angles in the antenna far-field region and example for an omnidirectional radiation pattern; *b*) 3-D E probes; *c*) electrical monopole as a helix for circularly-polarised E field

This distribution should be determined at a distance $r > R_{ffz}$; this condition restricts the applicability of the antenna as close as possible to a given radiator. For example, the considered above 2.45-GHz resonance dipole has a far-field-zone radius $R_{ffz} \sim 61.2$ mm (or $\sim 5\lambda_0$). Figure 9*a* presents one of the most spread radiation-pattern diagrams – the so-called "omnidirectional" diagram of the resonance dipole. This diagram means that the dipole has biggest sensitivity perpendicularly on its axis (along 0z), but can "detect" the E field practically from each directions excepting exactly the direction 0z. An important parameter is also the antenna beamwidth – the angle width of the radiation diagram at level –3dB from the maximum. The –3-dB beamwidth is a good measure of the "directivity" of an antenna. An pure isotropic radiation pattern does not exist. Thus, if the task is to measure the total E field in a given point, $E_\Sigma = \sqrt{E_x^2 + E_y^2 + E_z^2}$, 3-D dipoles or monopoles should be used – see examples in figure 9*b*.

The regular dipole is suitable for detection of E field with a linear polarization, when the travelling wave keeps one direction of his E-field. For the waves with circular polarization the end of the E-field vector describes a circle. The right-hand circular polarization RHCP is defined for transmitting antenna, when the E-field vector rotates clockwise (note, that due to the reciprocal principle the parameters of one passive antenna in transmitting or receiving regime are fully equal). Figure 9*c* shows an example for monopole with helix wire, suitable for measurement of circularly polarized E fields.

Another types of simple local field sensors are the elementary Huygens' apertures (see figure 6*c*). If the aperture area is small compared to λ_0^2, the radiation pattern is wide, practically without back lobe – figure 10*a*. As long the aperture diameter 2*a* increases, the radiation diagram becomes narrower, the antenna gain increases, but side lobes appear – see the example in figure 10*b* for circular horn antenna with radius $a = 3\lambda_0$. For very low frequency the dimension of similar apertures becomes extremely big. Figure 10*c* shows a useful solution – utilization of a pair of spherically curved E- and H-type dipoles, which acts like a quasi-Huygens aperture with very similar radiation diagram like the normal aperture. The aperture antennas – horns, reflectors, slot antennas, planar patches, lens antennas, etc. [4-5] are wide spread also like high-gain and high-efficiency field sensors, but they will not be discussed here.

3.2. Broad-band, ultra-wideband and frequency-independent sensors

The resonance thin-wire dipoles have narrow (~10-%) normalized bandwidth BW = $\Delta f/f_0$, where $\Delta f = f_2 - f_1$ is the difference between the frequencies $f_{1,2}$ for achieving of –10-dB return losses in the reflec-
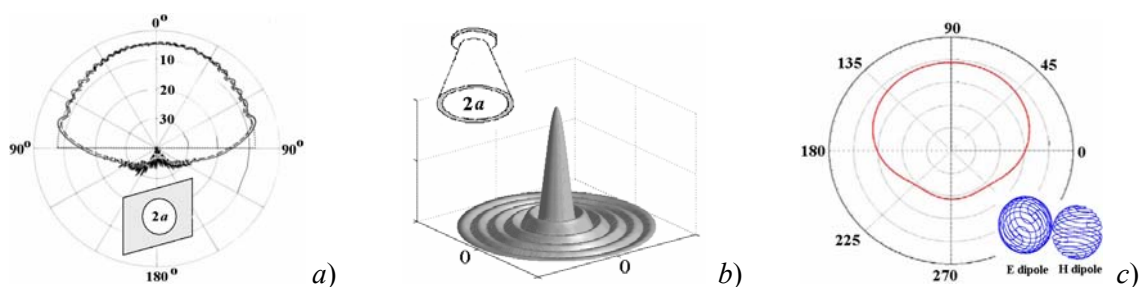

Figure 10. Radiating apertures [6]: *a*) radiation pattern of small circular aperture with radius $a = 0.42\lambda_0$; *b*) 3-D radiation pattern of circular horn with radius $a = 3\lambda_0$; *c*) imitation of a reduced-size quasi-Huygens source at very low frequency by a coupled pair of H and E curved dipoles and view of its radiation pattern.

ted from the antenna signal and f_0 is the central frequency determined by the dipole length. The reason of the narrow-band operation is the high quality factor of the considered $\lambda_0/2$-resonator; this behaviour is due to the strong coherent diffraction between the both wire ends [4]. In fact, the short dipole with length $D \langle\langle \lambda_0/2$ has much wider BW, but the radiation efficiency (and therefore, the sensor sensitivity) is very weak. One can increase the BW of the resonance dipole by using of more complex wire geometries – see figure 11a,b. The main reason for increasing of BW in these structures is the more complicated incoherent diffraction from the curved edges in these cases. Thus, the quality factor decreases and the BW become wider (for example the ratio f_2/f_1 becomes up to 2:1 and even 3:1 – figure 11c). The upper frequency limit of these constructions is determined by the parasitic excitation of high-order modes that causes pattern narrowing and multiple radiation lobes.

Another more effective way for achieving of ultra-wide band antenna operation is the adopting of frequency-independent (figure 12a,b) or frequency-scaled geometries (figure 12c,d). The log-periodic antenna is defined as a structure whose electrical properties vary periodically with the logarithm of the frequency and a multi-decade operation can be reached. In fact, the frequency independence occurs for a certain low-frequency cut-off (for which the longest tooth length is $\lambda_0/4$)

3.3. Traveling-wave sensors: surface-wave and leaky-wave probes

The considered above dipoles/monopoles are typical resonant field sensors, which operation is based on the formed standing waves in the fed wire conductors. The travelling-wave sensors have non-resonant action, based on an effective propagation of slow or fast waves along the antenna axis [5]. The slow-wave antennas ($v_{ph}/c < 1$) are based on the radiation of surface waves along delaying systems – dielectric rods, helixes, series of metal rods (Yagi-Uda antennas – see figure 12a), etc. Since the surface waves radiate only at discontinuities, nonuniformities and curvatures at the open interface, the total pattern of this "end-fire" type of antennas is formed by the interference between the feed lines and the end-terminal patterns. Usually the surface-wave antenna has narrow BW and limited gain (less than 20 dB) – see figure 12b. A very interesting solution for surface-wave E-field probe is the printed version, so-called quasi-Yagi antenna, which can be applied up to millimetre-wave range.

The leaky-wave antenna is basically a waveguiding structure that possesses a mechanism that permits it to leak power in a tilt direction all along its length during the propagation of fast waves ($v_{ph}/c > 1$).
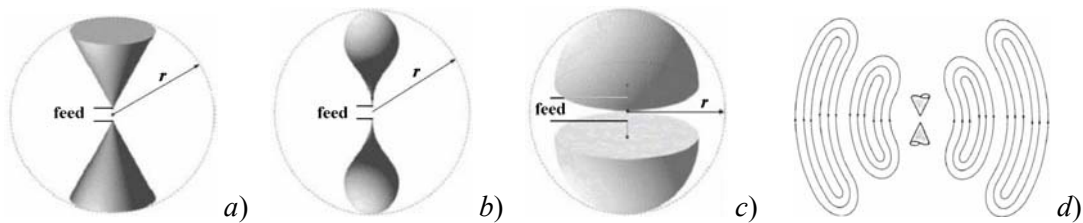

Figure 11. Broad-band dipoles: a) bi-conical; b) tapered (intermediate bandwidth BW); c) hemispherical BW (wide BW); d) the bi-conical dipole is very suitable for detection of quasi-spherical waves [4].
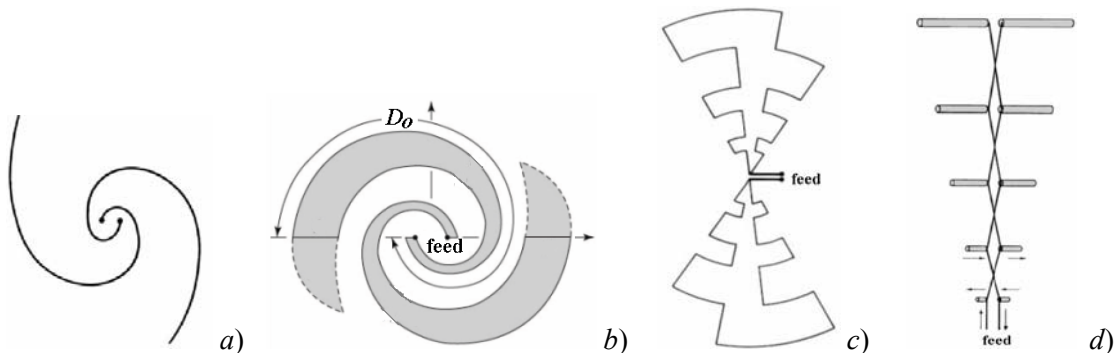

Figure 11. Ultra-wide band and frequency-independent dipoles: a) spiral dipole; b) planar spiral dipole; c) log-periodical antenna; d) log-periodical dipole with crisscross connection [4].
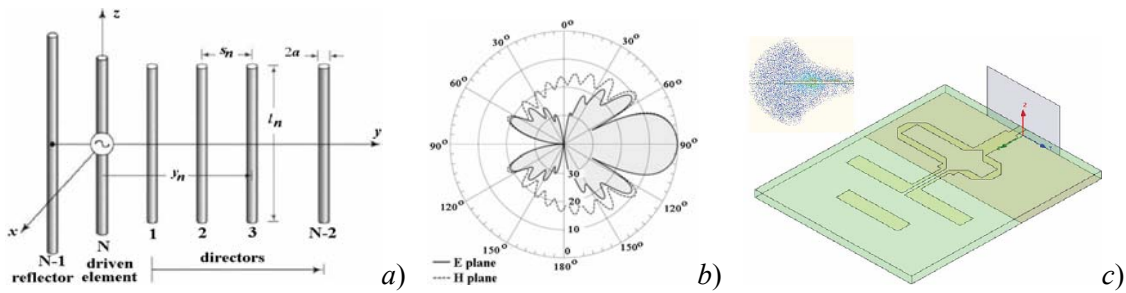
Figure 12. Travelling-wave dipoles: *a*) ordinary Yagi-Uda TV antenna; *b*) its radiation diagram; *c*) planar quasi-Yagi antenna – an effective sensor for detection or excitation of surface waves [4].

To be able to radiate effectively before its end, this antenna should be relatively long ($\sim 20\ \lambda_0$); the beamwidth of such antenna depends on the leakage constant and the beam direction depends on the frequency. Thus, the leaky-wave antenna can be scanned by varying the frequency. A typical example for leaky-wave antenna is the array of nonresonant slots in rectangular waveguides (not shown here).

3.4. Miniaturized sensors using fractals and metamaterials

The achieving of broadband operation is an important task for the E-field probes, but the other important task is the size miniaturization. The simplest way is the placing of the dipole in a dielectric body; the reducing factor is $1/\sqrt{\varepsilon_r}$; ε_r is the dielectric constant. The other way, especially at low frequencies, is the use of lumped LC elements. But there exist more efficient methods given below.

The utilization of the fractal geometry is one of the so-called natural-based antenna designs. In this case the miniaturization of the antennas is based on employing of the fractals [4, 5]. The original term "fractal" means broken or irregular fragments to describe a family of complex shapes that possess an inherent and self-similarity or self-affinity in their geometrical structures. Figure 13*a* shows how the known straight dipole could be reconstructed to the so-called Koch fractal dipole – it is composed from small but exact copies of itself. The results after the 5 stages is an increasing of the effective dipole length, nevertheless that the length of the straight line is equal in all the stages. Big 2-D sizes' reduction can be achieved with the Hilbert curve. It is an example of a space-filling fractal curve that is self-avoiding (i.e., has no intersection points) – see figure 13*b*. Used as GPS antenna the size can be minimized more than 3 times. Figure 13*c* shows the Sierpinski gasket dipole. Similar antenna elements
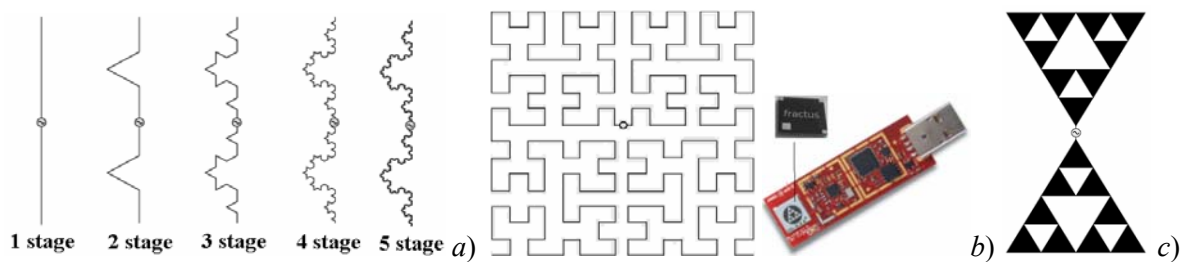

Figure 13. Miniaturised dipoles using fractals: *a*) Koch fractal dipole formed by 5 stages; *b*) Hilbert-curve dipole used for extremely small GPS antenna inserted into USB devices; *c*) Sierpinski's bow-tie dipole
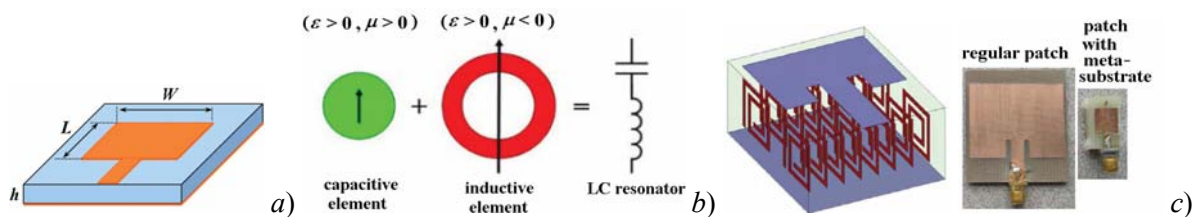

Figure 14. Miniaturised patches: *a*) ordinary microstrip patch; *b*) concept for using of metamaterials; *c*) miniaturized microstrip patch using embedded circuit metasubstrate compared with the original patch

have multiband operation; this is due to the many self-similar objects, which radiate in different frequency ranges. The main disadvantage of the fractal antennas is the decreased radiation efficiency.

The other attractive way for miniaturisation of the antenna dimensions is the using of the metamaterial filling. There are a variety of engineered electromagnetic materials [4], implemented into the antenna design. We will consider here only an example for using of embedded-circuit metasubstrates. The regular dielectrics and magnetodielectrics used in the antenna design have positive values of the dielectric and magnetic constants ($\varepsilon > 0$, $\mu > 0$). Plasmas ($\varepsilon < 0$, $\mu > 0$) and gyrotropic ferrites ($\varepsilon > 0$, $\mu < 0$) in external magnetic field can acquire negative values of one of the material constants. The materials with double negative material constants ($\varepsilon < 0$, $\mu < 0$) are not found in the nature, but can be physically realizable. How these materials can help for the miniaturization? The operation frequency of the microstrip patch made by regular dielectrics is $\sim 1/\sqrt{LC}$, where C is the element capacitance and the L is the small inductance (figure 14a,b). If the filling is a properly designed embedded-circuit metasubstrate, the absolute values of the effective material constants ($|\varepsilon|$ and especially $|\mu|$) can strongly increase, the corresponding element C and especially L increase, and the resonance frequency decrease. This means that for the same frequency the size of the microstrip patch is considerable smaller (more than 4 times) – see figure 14c. The radiation patterns of the both patches are similar but the BW of the patch with metasubstrate is wider.

3.5. Reconfigurable sensors. Plasma dipoles and patches

Let us finally consider the possibility to tune the operation frequency of the E-field sensors. One very efficient way to do reconfigurable antennas is the utilization of dc-controlled MEMS switches (Micro Electro-Mechanical System). Figure 15a,b gives an example for a planar reconfigurable monopole with 2 MEMS's ensuring 3 different effective wire lengths and operating at 3 different frequencies – figure 15c. The speed of the modern MEMS switches is high enough and this fact allows a relatively easy online tuning of the antenna frequency range, which is important for communication applications. The plasma antennas also have possibility to be tuneable – figure 16. There exist two main ways to construct reconfigurable plasma antenna. The first one is the changing of the effective dipole length by the control of the plasma discharge length (in this case the plasma column is used instead of the metal
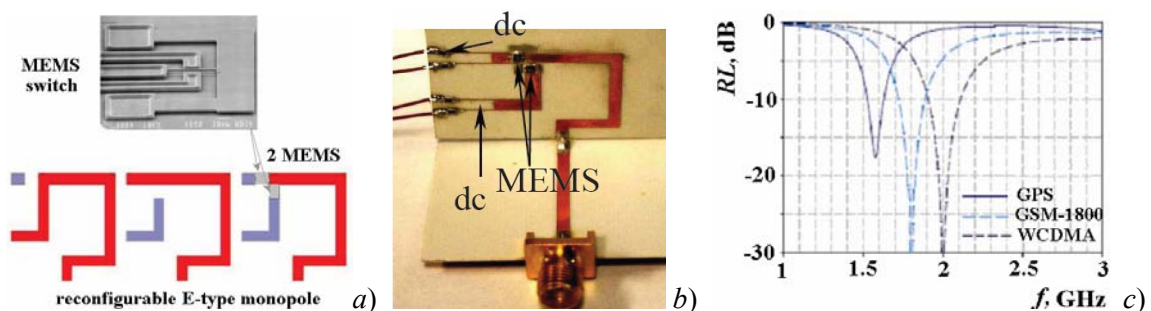

Figure 15. Reconfigurable E-field monopoles: *a*) Printed monopole with 2 MEMS for obtaining of three wire lengths; *b*) experimental monopole; *c*) measured return losses for the three cases
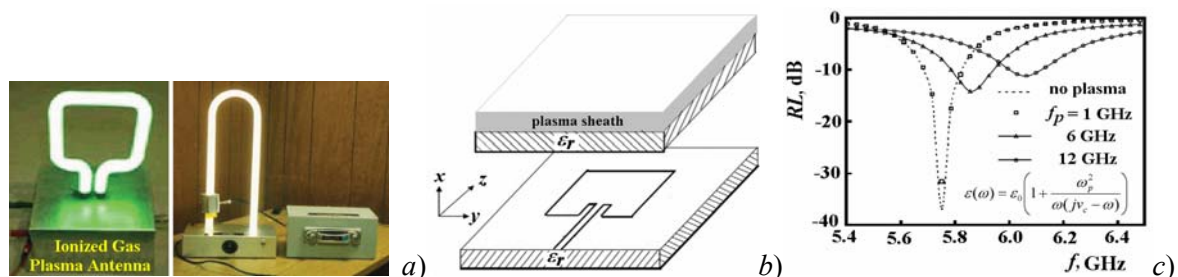

Figure 16. Plasma dipoles and patches: *a*) ionized gas plasma loops; *b*) microstrip patch with controlled plasma sheath; *c*) measured return losses of the microstrip plasma patch in the range 5.4-6.4 GHz
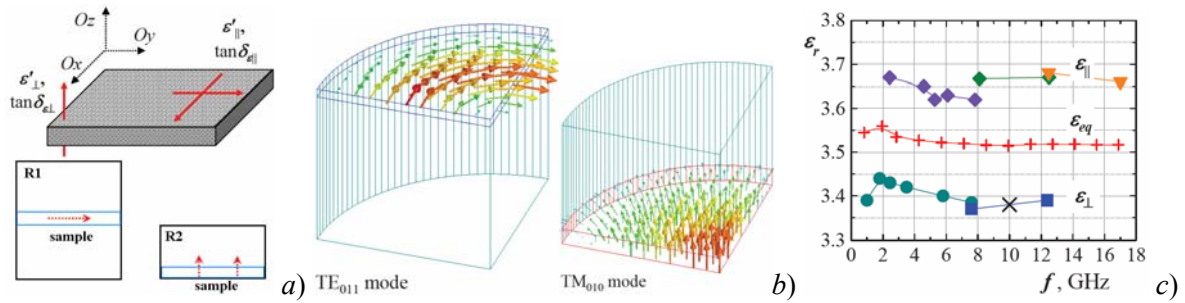
Figure 17. Substrate anisotropy: *a*) two-resonator method; *b*) E-field distribution of the considered modes; *c*) measured parallel, perpendicular and equivalent dielectric constant Ro4003 substrate by two-resonator method

wire). The second way is the using of the plasma medium as an electronically controlled metematerial. Figure 16*b* shows a simple construction – regular patch covered by plasma sheath. The operation frequency of the antenna can be changed by control of the plasma frequency – figure 16*c*.

4. Utilisation of 3D electromagnetic simulators for E-field measurement purposes

Finally, we briefly consider a specific, but important problem – the utilization of the EM simulators as assistant tool for microwave measurements, including the E-field measurements. The modern 3-D simulators, based of powerful EM methods [4] (FDTD, FEM, MoM, etc.) have great capability for accurate numerical simulations of very complicated EM structures. In fact, the modern style of design of the RF and antenna engineers is exactly based on the construction of extremely detailed structure models with expectations to achieve more accurate design. Similar approach is used with more or less success to do simulations, which support the measurement process in the microwave range. Contrariwise, we propose an opposite approach for application of the 3-D simulators for measurement purposes – construction of stylized 3-D models without unnecessary elements (connectors, excitation loops or probes, tuning elements, etc.), which ensure simplicity, accuracy and computer time and memory efficiency. In order to be more concrete, we present two examples.

4.1 Example 1 – determination of dielectric substrate anisotropy using two-resonator method
The modern RF substrates used in the electronics have well expressed dielectric anisotropy – different dielectric parameters (dielectric constant ε_r and dielectric loss tangent $\tan\delta_\varepsilon$) parallel and normal to the substrate surface – figure 17*a*. The anisotropy is not included into the manufacturer catalogues; this fact is very inconvenient for many RF and antenna designers, which want to do more accurate design. Due to this reason we developed the two-resonator method [7] for measurement of the dielectric anisotropy of multilayer materials. This method employs two resonators, which support modes with appropriate orientation of the E fields in order to determine the necessary parameters parallel and perpendicular to the substrate surface. For this purpose we use 3-D simulators to support the measurements. Figure 17*b* shows the simulated E-field distribution for two simple cases – for TE_{011} mode in the first cylindrical resonator R1 (the E field is parallel to the sample surface) and for TM_{010} mode in the second resonator R2 (the E field is normal to the sample surface). The presented pictures illustrate the used style for construction of the 3-D resonator models. They have been built as pure cylindrical and plane surfaces without any coupling details. In order to ensure coincidence between the measured and calculated resonance parameters (frequency and Q factor) of pure (without sample) resonators equivalent parameters have been introduced – equivalent diameters and equivalent wall conductivity. Fast simulations can be realized, if the whole resonators have been splitted and only symmetrical parts of the resonator have been simulated (1/8 R1 and 1/4 R2) using appropriate magnetic-wall boundary conditions – "E-field symmetry" (if the E field is parallel to the surface) or "H-field symmetry" (if the E field is perpendicular to the surface). Finally, the simulations of the resonators with samples easy give the dielectric parameters. This approach ensures both accuracy and fast simulations, and the measurement errors are kept quite low, ±3 % for ε_r and ±7 % for $\tan\delta_\varepsilon$. An example for the measured dielectric constant anisotropy is shown in figure 17*c* for one of the most popular RF substrate Ro4003.
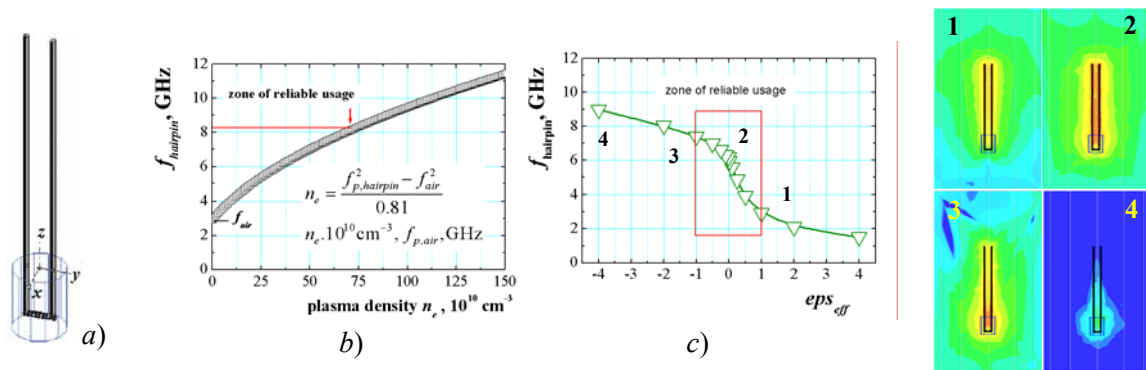
Figure 18. Hairpin resonator as a microwave probe for determination of the plasma density: *a*) 3-D model; *b*) dependence of the hairpin resonance frequency v/s the plasma density; *c*) dependence of the resonance frequency v/s the effective plasma permittivity and simulated E-field distributions in 4 different points

4.2 Example 3 – sensitivity of the hairpin resonance probe for determination of plasma density
The hairpin resonator can be used as a very effective E-field probe for determination of the plasma density – figure 18. The main benefit of this method is that the measurements are based on determination of the resonance frequency f_{haipin} instead of any absolute measurements of E-filed magnitudes, which ensure better sensitivity, accuracy and measurement simplicity. The hairpin probe is a quarter-wave two-wire resonator, which can be relatively easy designed for TEM-mode operation [9]. The open end of the structure has maximum of the E field of the standing wave, which makes this resonance probe enough sensitive to the changes of the dielectric parameters of the surrounding medium – the plasma media in this case. The opposite short end has maximum of the H field, which allows to construct quite stable and reliable coupling between the resonator and the feed coaxial cable using H-type loop probe (figure 6*b*). But how to determine the measurement sensitivity of this resonance probe? For this purpose we construct a simplified 3-D model of the hairpin resonator with a small ceramic support at the short end without introducing the coupling loop model – figure 18*a*. Then we simulate this structure for different effective dielectric constant of the plasma medium (ε_{eff} in the interval from 4 to –4). The results have been presented in figure 18*c*. We can see that the measurement sensitivity is higher (the curve slope in bigger) in the interval $\varepsilon_r \subseteq (1, -1)$. Moreover, the E-field distributions in several specific points (1-4) over the plotted curve have been given, which confirm the loss of sensitivity of the hairpin probe for $|\varepsilon_{eff}| > 1$. In these points (3, 4) the maximum of the E filed of the standing wave changes from the open end (when $\varepsilon_{eff} > 0$) to the short end (due to the negative sign of ε_{eff}) and the probe does not more react to the dielectric constant changes.

5. References
[1] "Handbook of Electromagnetic Compatibility", Ed. by Perez R, Academic Press Inc., 1995
[2] Agilent® Application Note 1449-1/2/3/4 " Fundamentals of RF and Microwave Power Measurements"; Agilent® Application Note 150-1 "Spectrum Analysis. Amplitude and Frequency Modulations"; on-line: www.agilent.com
[3] "Free-space measurement seminar", June 2005, Agilent Technology "; on-line: www.agilent.com
[4] "Modern Antenna Handbook", Ed. By Balanis C A, John Wiley & Sons Inc., 2008
[5] "Antenna Engineering Handbook", Ed. By Volakis J, McGraw-Hill Co., 2007
[6] Orfanidis S J, "EM Waves and Antennas", on-line: www.ece.rutgers.edu/~orfanidi/ewa
[7] Dankov P I 2006 "Two-Resonator Method for Measurement of Dielectric Anisotropy in Multi-Layer Samples" *IEEE Trans. on MTT* **54** 1534-44
[8] Dankov P I, Stefanov P, Gueorguiev V and Ivanov T 2010 Hairpin-Resonator Probe and Measurement Considerations *J. Phys.: Conf. Ser.* **207** 202-9